Vol 16 No 11, November 2007
1009-1963/2007/16(11)/3507-07
Chinese Physics
© 2007 Chin. Phys. Soc.
and IOP Publishing Ltd

Electronic transport through an open elliptic cavity*

Wang Zhe-Xian(王哲献)[a)], Ming Yi(明 燚)[b)], and Ding Ze-Jun(丁泽军)[a)†]

[a)] *Hefei National Laboratory for Physical Sciences at Microscale and Department of Physics, University of Science and Technology of China, Hefei* 230026, *China*

[b)] *Department of Physics, Anhui University, Hefei* 230039, *China*

(Received 7 March 2007; revised manuscript received 21 March 2007)

This paper computes the conductance of an open ellipse cavity and discusses the effect of finite leads on conductance. The lead introduces mode coupling with bound states in the cavity which contributes to Fano resonant line shapes in conductance. By examining the resonant states in the cavity, the effects of state mixing and annular probability distribution of wave function due to the presence of leads are found. The results have been compared with the transport properties of other systems. The finite leads result in two effects, i.e. the evanescent mode contribution and additional oscillations, to the conductance.

Keywords: open elliptic cavity, mode coupling, finite leads, transport
PACC: 7335, 7210, 7320D, 0365G

1. Introduction

Modern technology enables fabrication of devices of sizes comparable with the mean free path of electrons. In this regime, electrons can move ballistically. In the last two decades, the transport properties of ballistic microstructures especially the transport properties of quantum dots[1,2] have gained much attentions. A number of theoretical models were given to study transport properties through quantum dots of different structures, for instance, a rectangle connected with two perfect channels,[3−11] a stadium with oppositely-aligned leads,[12] a circle with two conical leads,[13,14] or other structures.[15−23] Elliptical system is a very important structure, there have been many calculations of energy levels or confined states in elliptic dot,[24−26] but to our knowledge, the transport properties of the elliptic billiard have not been studied yet.

In this paper we study the conductance of elliptic dot, and, the probability distributions for revealing transport properties more intuitively. Furthermore, we focus the attention on a more realistic system which composed of an open cavity and two finite leads, and discuss the effect of finite leads on the conductance.

2. Theoretical model

A sketch of the structure considered here is illustrated in Fig.1(a). The device consists of an elliptic cavity and two straight channels. Electrons are confined in a very thin layer in z-direction, so we just need to consider transport in two-dimensional plane. Electrons move along the x-axis and we assume a hard wall potential in the y-direction. Inside the channel the potential is set to zero for simplicity. One-electron approximation is adopted in this calculation.

For this two-dimensional system, the Schrödinger equation is

$$\Big[-\frac{\hbar^2}{2m^*}\Big(\frac{\partial^2}{\partial x^2}+\frac{\partial^2}{\partial y^2}\Big)+V_{\rm c}(x,y)\Big]\psi(x,y)=E\psi(x,y), \quad (1)$$

where m^* is the electron effective mass, $V_{\rm c}(x,y)$ is the lateral confining potential, and E is the energy of the incident electrons. We solve this equation with a scattering matrix technique.[16] The device is divided into many strips along x-axis, and the wave function in the pth strip is written as

$$\psi^p(x,y)=\sum_n\Big[a_n^p{\rm e}^{{\rm i}k_n^p(x-x_p)}+b_n^p{\rm e}^{-{\rm i}k_n^p(x-x_p)}\Big]\,\varphi_n^p(y),$$

$$\varphi_n^p(y)=\sqrt{\frac{2}{D^p}}\sin\Big[\frac{n\pi}{D^p}\Big(y+\frac{D^p}{2}\Big)\Big], \quad (2)$$

where D^p is the width of the pth strip. The longitudinal wave number is given by $k_n^p=\sqrt{2m^*E/\hbar^2-(n\pi/D^p)^2}$, which can be either real or imaginary. An imaginary k_n^p is related to the evanescent mode in the channel. At the interface of the pth and $(p+1)$th strip, the coefficients of the wave function in the two strips may be represented by column

*Project supported by the National Natural Science Foundation of China (Grant Nos 10574121, 90406024 and 10025420), Chinese Education Ministry and Chinese Academy of Sciences.
†Corresponding author. E-mail: zjding@ustc.edu.cn

vectors $(A^p, B^p)^{\mathrm{T}}$ and $(A^{p+1}, B^{p+1})^{\mathrm{T}}$. They are related by a scattering matrix S^p, namely:

$$\begin{bmatrix} B^p \\ A^{p+1} \end{bmatrix} = \begin{bmatrix} S^p_{11} & S^p_{12} \\ S^p_{21} & S^p_{22} \end{bmatrix} \begin{bmatrix} A^p \\ B^{p+1} \end{bmatrix}. \tag{3}$$

The continuity of the wave function and their first derivatives at the interface (assuming $x = 0$) gives out the following matrix equations:

$$\begin{aligned} &D^{\mathrm{T}}(A^p + B^p) = A^{p+1} + B^{p+1}, \\ &K^p(A^p - B^p) = DK^{p+1}(A^{p+1} - B^{p+1}), \end{aligned} \tag{4}$$

where D is a matrix with element D_{mn} given by $D_{mn} = \int \varphi^p_m(y)\varphi^p_n(y)\mathrm{d}y$, and K^p is a diagonal matrix with $(K^p)_{mm} = k^p_m$. Solving these two equations we can obtain the scattering matrix S^p. The total scattering matrix S should be obtained by composing the scattering matrices in each strip. Finally, we obtain the conductance by using the linear conductance formula

$$G = \frac{2e^2}{h}\sum_{m,n} T_{mn} = \frac{2e^2}{h}\sum_{m,n}(S_{21})_{mn}. \tag{5}$$

T_{mn} in Eq.(5) indicates the probability of the electrons incident from left channel n while transmitting to the right channel m. The sum runs over all the propagating modes in the wire.

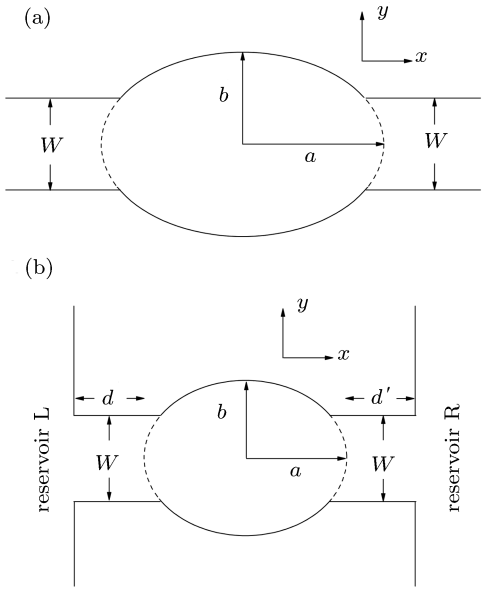


Fig.1. Schematic view of the system. (a) An open elliptic dot connects with two infinite long leads. (b) An open elliptic dot connects to external electron reservoir with two leads of finite lengths.

Lunderberg[27] has studied a finite leads system by using the transfer matrix method with Kirczenow's model;[28] however, the transfer matrix method is known to be unstable. Here we combine the Kirczenow model[28] with the scattering matrix technique,[16] enabling us to study complex structures of cavity. Figure 1(b) shows the structure of an elliptic cavity connected to reservoir by two leads of finite lengths. Inside the channel, we can still write the wavefunction in the form of that in Eq.(2). But in the reservoir, we need to rewrite the wave function. For an electron with wave vector $k = (k_x, k_y)$ and energy E, the wave functions of the left and right reservoir are written as follows:

$$\begin{aligned} \psi^{\mathrm{L}}_k &= \mathrm{e}^{\mathrm{i}k_x x + \mathrm{i}k_y y} + \int_{-\infty}^{+\infty} b^{\mathrm{L}}_{k'_y} \mathrm{e}^{-\mathrm{i}k'_x x + \mathrm{i}k'_y y}\mathrm{d}k'_y, \\ \psi^{\mathrm{R}}_k &= \int_{-\infty}^{+\infty} a^{\mathrm{R}}_{k'_y} \mathrm{e}^{\mathrm{i}k'_x x + \mathrm{i}k'_y y}\mathrm{d}k'_y, \end{aligned} \tag{6}$$

where $k = k' = \sqrt{2m^*E}$. Again, applying the matching method for the wave functions and their first derivatives at the two ends, we obtain a group of equations:

$$\begin{aligned} &\begin{pmatrix} S^1_+ & S^1_- \\ 0 & 0 \end{pmatrix}\begin{pmatrix} A^1 \\ B^1 \end{pmatrix} + \begin{pmatrix} 0 & 0 \\ S^N_- & S^N_+ \end{pmatrix}\begin{pmatrix} A^N \\ B^N \end{pmatrix} \\ &= \begin{pmatrix} \Lambda^1 \\ 0 \end{pmatrix}, \end{aligned} \tag{7}$$

where (A^1, B^1) and (A^N, B^N) are coefficients of wave functions in the first strip (left end) and the Nth strip (right end) of channel respectively. Other variables in the first strip are defined as

$$\begin{aligned} (S^1_\pm)_{mn} &= [T_{mn} \pm k_n\delta_{mn}w/2]\mathrm{e}^{\mp \mathrm{i}k_n d}, \\ \Lambda^1_m &= 2\mathrm{i}k_x \mathrm{e}^{-\mathrm{i}k_x d} M_{k_y,m}, \\ T_{mn} &= \mathrm{i}\int_{-\infty}^{+\infty} \frac{\mathrm{d}k'_y}{2\pi}\, k'_x M_{k'_y,m} M_{-k'_y,n}, \\ M_{k,n} &= \int_{-w/2}^{+w/2} \sin\Big[\frac{n\pi}{w}\Big(y + \frac{w}{2}\Big)\Big]\, \mathrm{e}^{\mathrm{i}ky}\mathrm{d}y, \end{aligned} \tag{8}$$

where w is the width of the first strip and k_n is the same as that defined previously. The variables in the Nth strip can be obtained by correspondingly changing the parameters of the first strip into the Nth strip in Eq.(8).

According to the scattering matrix, the relation between coefficient (A^1, B^1) and (A^N, B^N) are

$$\begin{bmatrix} B^1 \\ A^N \end{bmatrix} = \begin{bmatrix} S_{11} & S_{12} \\ S_{21} & S_{22} \end{bmatrix} \begin{bmatrix} A^1 \\ B^N \end{bmatrix}. \tag{9}$$

Here S is the scattering matrix. Substituting Eq.(9) into Eq.(7), we have

$$\begin{pmatrix} S^1_+ + S^1_- S_{11} & S^1_- S_{12} \\ S^N_- S_{21} & S^N_- S_{22} + S^N_+ \end{pmatrix}\begin{pmatrix} A^1 \\ B^N \end{pmatrix} = \begin{pmatrix} \Lambda^1 \\ 0 \end{pmatrix}. \tag{10}$$

Solving the equations we can obtain (A^1, B^1), and then (A^N, B^N). The conductance contributed by electrons incident from all the angles can be written as

$$\begin{aligned} G &= \frac{2e^2}{h}\int_{-\pi/2}^{+\pi/2}\mathrm{d}\phi\int_{-w/2}^{+w/2}2j_x(k)\mathrm{d}y \\ &= -\int_{-\pi/2}^{+\pi/2}\mathrm{d}\phi\int_{-w/2}^{+w/2}2 \\ &\quad\times\mathrm{Re}\Big[\psi^*(x,y)\mathrm{i}\frac{\partial}{\partial x}\psi(x,y)\Big]\mathrm{d}y, \end{aligned} \tag{11}$$

where ϕ is the angle between the incident wave vector k and the x-axis.

3. Eigenstates in elliptic dot

The energy levels and eigenstates of a closed elliptic dot are obtained by solving the Schrödinger equation in elliptical coordinates, with a hard wall confinement at the boundary, i.e. $V = \infty$ when $(x/a)^2 + (y/b)^2 \geq 1$. Applying the coordinate transformation, $x = f\cosh u\cos\upsilon$, $0 \leq u \leq \infty$, $y = f\sinh u\sin\upsilon$, $0 \leq \upsilon \leq 2\pi$, where $f = \sqrt{a^2+b^2}$ is the focal length, from Eq.(1) we obtain[24]

$$\begin{aligned} &\frac{\partial^2\Psi}{\partial u^2} + \frac{\partial^2\Psi}{\partial\upsilon^2} + \frac{f^2k^2}{2}\cosh(2u)\Psi \\ &- \frac{f^2k^2}{2}\cos(2\upsilon)\Psi = 0. \end{aligned} \tag{12}$$

The electron momentum k is defined by $k^2 = 2m^*(E - V_\mathrm{c})/\hbar^2$. Let a solution be $\Psi(u,\upsilon) = F(u)G(\upsilon)$ and define $q = f^2k^2/4$, then substituting $\Psi(u,\upsilon)$ into Eq.(12) we obtain

$$\frac{\mathrm{d}^2F(u)}{\mathrm{d}u^2} - (c - 2q\cosh(2u))F(u) = 0, \tag{13}$$

$$\frac{\mathrm{d}^2G(\upsilon)}{\mathrm{d}\upsilon^2} + (c - 2q\cos(2\upsilon))G(\upsilon) = 0, \tag{14}$$

where c is the separation constant. Equation (13) is known as the radial Mathieu equation, and Eq.(14) the angular Mathieu equation. The solutions of these equations are[24]

$$\begin{aligned} G_l(\upsilon,q) &= \begin{cases} ce_l(\upsilon,q), \\ se_l(\upsilon,q), \end{cases} \\ F_l(u<U,q) &= \begin{cases} Mc_l^{(1)}(u,q), \\ Ms_l^{(1)}(u,q), \end{cases} \end{aligned} \tag{15}$$

where $l = 0, 1, 2, \cdots$. $(u = U, \upsilon)$ denotes coordinates of the border of an elliptic dot; $u = U$ is the radial distance of the border from the centre of the elliptic dot. The normalization factors are not included here. The Mathieu functions $ce_l(\upsilon,q)$, $se_l(\upsilon,q)$ are the first kind solutions of the angular Mathieu equation and are even and odd respectively. For radial solutions, $Mc_l^{(1)}(u,q), Ms_l^{(1)}(u,q)$, they are the first kind solutions of the radial Mathieu equation and are also even and odd respectively. Solving the boundary condition $\Psi(u,\upsilon)|_{u=U} = 0$ we obtain the eigen energy levels and then the eigenstates of the dot. The eigenstate can be expressed as $(N,l)^{\mathrm{e(o)}}$, in which N indicates the Nth energy level, l is the order and e(o) means that the solution has even (odd) symmetry. N and l relate, respectively, to the number of latitudinal and longitudinal nodes of the wave function.

4. Numerical results

In this section, the conductance as a function of electron energy will be presented. In our discussion, five or more evanescent modes are involved for each strip, and we take the number of incident transport modes to be one and the effective mass for GaAs to be $m^* = 0.067\ m_\mathrm{e}$. It is sufficient to set the number of divided segments be larger than 50.

4.1. Infinite channels

We begin with the case of an elliptic cavity connected two infinite channels. Figs.2(a)–2(c) show the conductance as a function of energy for different parameters of cavity. The energy interval we concern is between the two lowest propagating modes $E_1 = 56.12$ and $E_2 = 224.50$ meV, in which only the first transport mode is stimulated. Each curve shown in Fig.2 is full of the conductance fluctuations, especially for the third case.

Considering Fig.2(a), for example, we find that the curve consists of a plateau and many vertical lines. These vertical lines are all of Fano resonance line shapes, they are too narrow to be resolved in the figure. Fano resonance in waveguide systems can be interpreted as a result of the coupling between the bound states (eigenstates) in the cavity and the continuum states (propagating modes) in the lead,[5] the decay rate of bound state and the peak width lie on the coupling strength. In Fig.3 we plot the probability distributions of wave functions at the energies $E_\mathrm{F} = 127.07$ and $E_\mathrm{F} = 205.47$ meV where the conductance are dips, and compare them with the eigenstates $(2,6)^\mathrm{e}$ and $(3,3)^\mathrm{e}$ of the elliptic dot of the eigenener-

gies $E = 127.07$ and $E = 205.47$ meV respectively. The close connection between the probability distribution of wave function and the eigenstate reveals the contribution of bound states to the conductance.

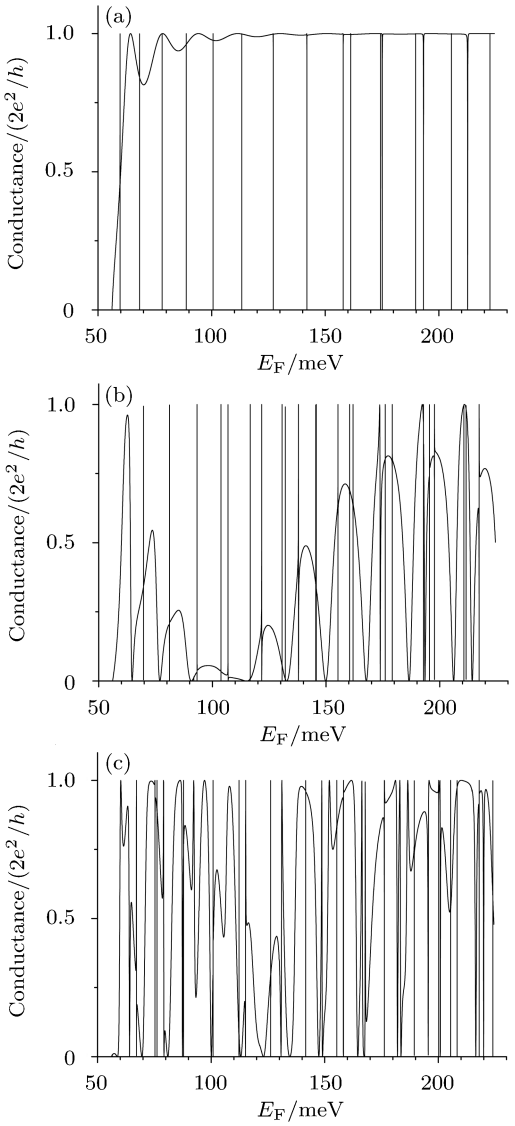


Fig.2. Calculated conductance as a function of the Fermi energy. The width of the leads is kept as a constant, $W = 10$ nm, while other parameters of the elliptic dot are different: (a) $a = 45$, $b = 15$ nm; (b) $a = 45$, $b = 30$ nm; (c) $a = 45$, $b = 40$ nm.

All the Fano resonance line shapes shown in Fig.2(a) can be related to eigenstates of $(2, l)^{\mathrm{e}}$, $l = 0 - 11$, and $(3, l)^{\mathrm{e}}$, $l = 0 - 4$, namely, only even symmetrical states in the dot are excited by the incident electrons. This is due to the symmetry between the leads and the cavity. The coupling between lead and cavity is given by the integral of the product of mode function in the lead and the cavity. If the product is odd symmetrical along y-direction then the integral is zero and there is no coupling. So the first propagating mode in the lead can only couple with modes which are even symmetrical along y-direction. If we include the second transport mode in the calculation then odd symmetrical states will affect the conductance as well.

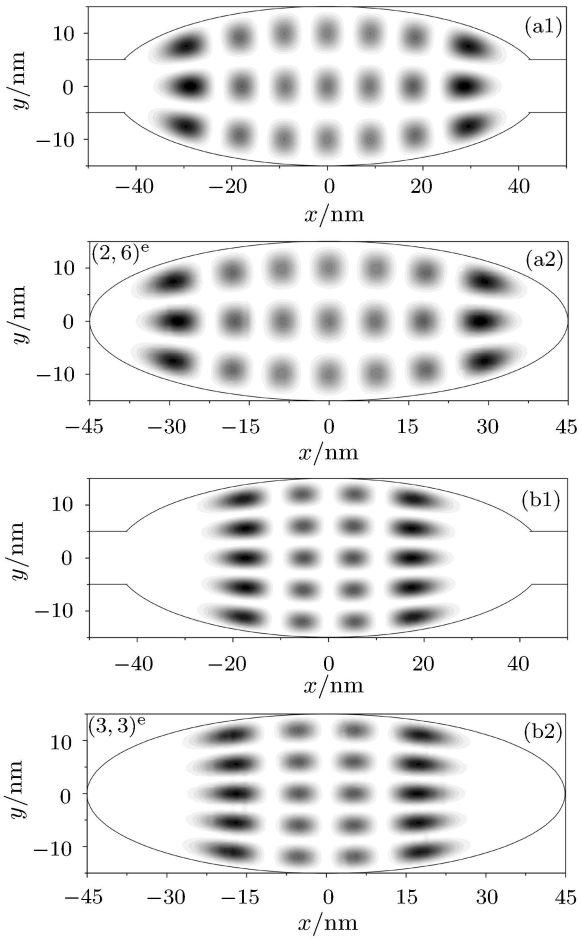


Fig.3. Probability distribution of wavefunctions and the corresponding eigenstates, the darker shading represents larger amplitude. The parameters of the device are $W = 10$, $a = 45$, $b = 15$ nm. (a) Probability distribution of wave function for energy $E_{\mathrm{F}} = 127.07$ meV (a1) and of the eigenstate $(2, 6)^{\mathrm{e}}$ for energy $E = 127.07$ meV (a2). (b) Probability distribution of wave function for energy $E_{\mathrm{F}} = 205.47$ meV (b1) and of the eigenstate $(3, 3)^{\mathrm{e}}$ for energy $E = 205.47$ meV (b2).

With the increase of the short axis of the elliptic cavity, the incident electrons with given latitudinal energy can excite more latitudinal modes in the dot, i.e., more eigen modes in the dot can couple with the propagating mode in the lead. Therefore, in Figs.2(b) and 2(c), the conductance becomes more complex as the parameter b increases.

In previous works,[8,10−13] state mixing due to the presence of leads is found in different shapes of dots. We can also find this interesting phenomenon in our

model. Figure 4(a) shows the elliptical probability distribution at the dip for energy $E_F = 183.57$ meV. This state does not relate to any single eigenstate of the dot, but a mixture of them. The energy $E_F = 183.57$ meV implies two possible states, $(1,19)^e$ and $(3,12)^e$ with energies of $E = 185.95$ and $E = 187.50$ meV respectively. A direct superposition of these two states leads to a distribution shown in Fig.4(b) which is similar to Fig.4(a), confirming that the state is to a some extent a mixing of $(1,19)^e$ and $(3,12)^e$. The elliptical probability distribution in Fig.4 which is analogous with the result given by Berggren *et al*[13] makes one to expect observing Aharonov–Bohm oscillations at low fields.

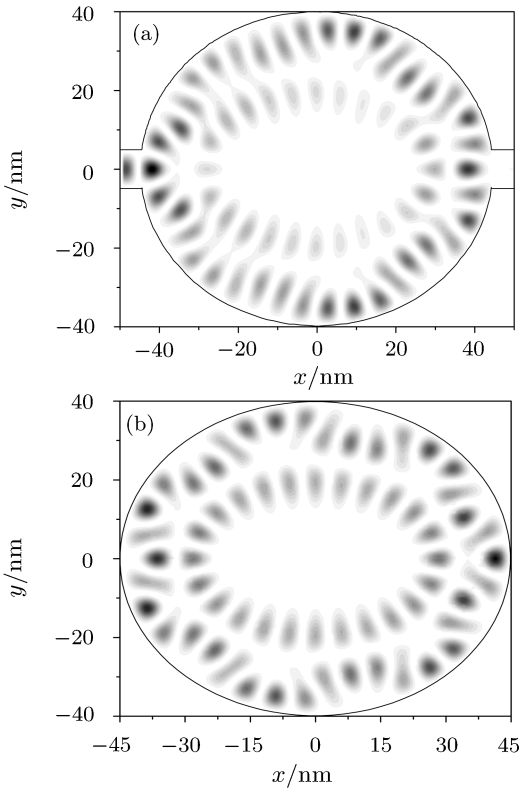


Fig.4. (a) Probability distribution of wavefunction for parameters, $W = 10$, $a = 45$, $b = 40$ nm and energy $E_F = 183.57$ meV. (b) Directly superposition of eigenstates $(1,19)^e$ and $(3,12)^e$ for energies of $E = 185.95$ and $E = 187.50$ meV.

4.2. Finite leads

We now turn to consider a system with finite leads. From a practical point of view, all experimental measurements are done with finite leads. An open dot connected with two finite leads is then more close to realistic conditions. Moreover, it is also an important question to find out the effect of the finite lead on the conductance.

The calculated conductance for a finite channel structure shown in Fig.1(b) is displayed in Fig.5(a) for different lead lengths. One can notice that for finite leads the conductance is different from the case of infinite channel shown in Fig.2(a) in two respects: many new resonant peaks appear with some additional oscillations superimposed on the plateau. This has been stated by Yuan and Gu[17] here we discuss them in detail.

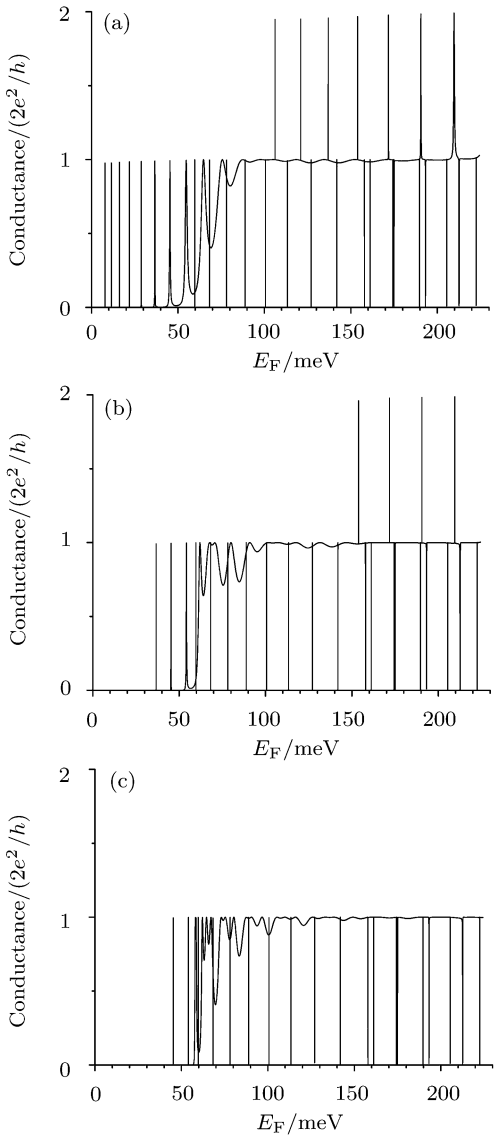


Fig.5. Conductance versus energy E_F for the device shown in Fig.1(b) with $W = 10$, $a = 45$, $b = 15$ nm but for different lead lengths: (a) $d = d' = 5$ nm; (b) $d = d' = 15$ nm; (c) $d = d' = 45$ nm.

These new resonant peaks are related to the evanescent mode in the lead coupling with the dot, or simply they are due to resonant tunnelling via quasibound states in the cavity.[3] In Figs.5(a)–5(c), as

the length of the leads increases, more resonant peaks disappear and the peaks become narrower. The reason for this is the evanescent modes in the lead can only stretch a certain distance; it affects the conductance when the lead is short but does not for enough long leads. Moreover, the width of the resonant peaks is proportional to the inverse lifetime or decay rate of a quasibound state in the cavity.[5] Increasing the lead length makes the quasibound states decay more slowly and prolongs their lifetimes, and then the peaks become narrower. The peaks appear below the first cutoff energy $E_1 = 56.12$ meV are due to the mode coupling between the first evanescent mode in the lead and the eigen mode in the cavity, and they are related to even symmetrical eigenstates. While, for the peaks imposed on the first quantized plateau, they are due to the contribution of the second evanescent mode in the lead, so all the eigenstates correspond to them are odd symmetrical.

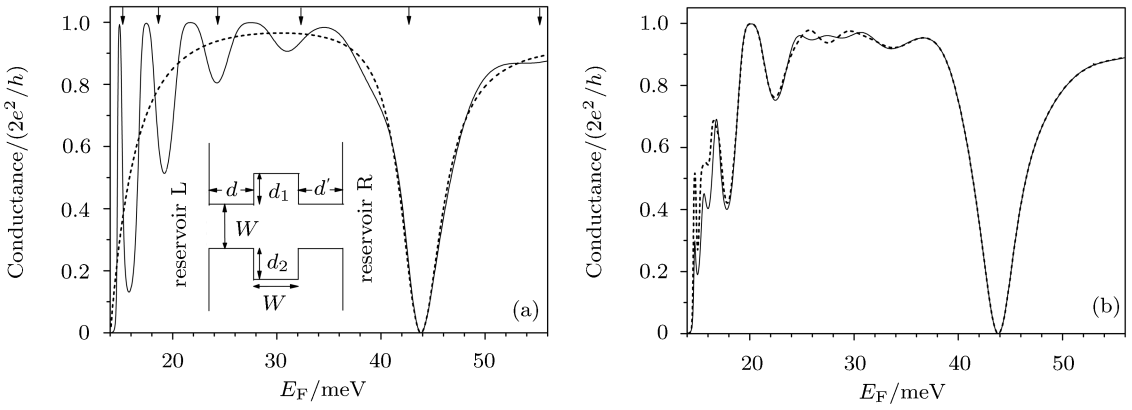


Fig.6. Conductance versus energy for the cross structure of $W = 20$, $d_1 = d_2 = 10$ nm and different lead lengths: (a) The dash line is for the cross structure with infinite long leads and the solid line is for the device with lead length $d = d' = 70$ nm. The arrows mark the values of energy E_F that satisfies the resonance condition, $i\lambda_x = 2d$ $(i = 1, 2, \cdots, 6)$, where $\lambda_x = h/\sqrt{2m^* E_F - \hbar^2(\pi/W)^2}$; (b) The solid line corresponds to an asymmetrical device with lead lengths $d = 80$ nm, $d' = 50$ nm. The dash line is an averaging of the conductance for devices with $d = d' = 50$ nm and $d = d' = 80$ nm.

Now we consider the character for additional oscillations superimposed on the plateau. In order to reveal the origin of these oscillations more directly, the conductance for a simple cross structure with infinite and finite leads is shown in Fig.6. For symmetrical leads configuration shown in Fig.6(a), the additional oscillations due to finite leads are quite in accord with the oscillation period indicated by arrows. So we can deduce that these oscillations are associated with the transverse length of the lead at both sides. In Fig.6(b), we compare the conductance of asymmetrical leads configuration with an average value of conductance of two symmetrical leads configurations. The consistency between two curves indicates that the additional oscillations in the conductance of asymmetrical leads configuration are due to the overlapping of oscillations originated from the resonance in leads at both sides. Based on this result, one can understand that the additional oscillations intensify when the leads become longer in Figs.5(a)–5(c).

5. Conclusions

In summary, we have studied the transport properties of an open elliptic dot and the effect of the finite leads on the conductance. Using the scattering matrix method we have calculated the conductance of open elliptic dot for different parameters. We have shown that the complex resonant peaks and dips in the conductance are due to the coupling between the mode in the lead and the eigenstate in the dot. We have also found the state mixing and annual probability distribution of wave function which have been noted by Berggren *et al*[3] in an open circular dot. The effect of the finite leads to the conductance is introducing the contribution of evanescent mode to the conductance and imposing additional oscillations on the conductance plateau. The additional oscillations are mainly related to the length of leads at both sides of a device.

References

[1] Kouwenhoven L P, Marcus C M, Mceuen P L, Tarucha S, Westervelt R M and Wingreen N S In: Kouwenhoven L P, Schön G and Sohn L L (ed) 1997 *Proceedings of the Advanced Study Institute on Mesoscopic Electron Transport* (Dordrecht: Kluwer)

[2] Bird J P, Akis R, Ferry D K, A P S de Moura, Lai Y C and Indlekofer K M 2003 *Rep. Prog. Phys.* **66** 583

[3] Berggren K F and Ji Z L 1991 *Phys. Rev.* B **43** 4760

[4] Iton T, Sano N and Yoshii A 1992 *Phys. Rev.* B **45** 14131

[5] Na K and Reichl L E 1998 *J. Stat. Phys.* **92** 519

[6] Na K and Reichl L E 1999 *Phys. Rev.* B **59** 13073

[7] Akis R, Ferry D K and Bird J P 1996 *Phys. Rev.* B **54** 17705

[8] Zozoulenko I V, Schuster R, Berggren K F and Ensslin K 1997 *Phys. Rev.* B **55** 10209

[9] Wang Y, Zhu N, Wang J and Guo H 1996 *Phys. Rev.* B **53** 16408

[10] Zozoulenko I V and Berggren K F 1997 *Phys. Rev.* B **56** 6931

[11] Sadreev A F 2004 *Phys. Rev.* E **70** 016208

[12] Akis R, Bird J P and Ferry D K 2002 *Appl. Phys. Lett.* **81** 129

[13] Berggren K F, Ji Z L and Lundberg T 1996 *Phys. Rev.* B **54** 11612

[14] Ree S and Reichl L E 1999 *Phys. Rev.* B **59** 8163

[15] Nakazato K and Blaikie R J 1991 *J. Phys.: Condens. Matter* **3** 5729

[16] Sheng W D 1997 *J. Phys.: Condens. Matter* **9** 8369

[17] Yuan S Q and Gu B Y 1993 *J. Appl. Phys.* **73** 7496

[18] Christensson L, Linke C H, Omling P, Lindelof P F, Zozoulenko I V and Berggren K F 1998 *Phys. Rev.* B **57** 12306

[19] Akguc G B and Reichl L E 2000 *J. Stat. Phys.* **98** 813

[20] Fuchss K, Ree S and Reichl L E 2000 *Phys. Rev.* E **63** 016214

[21] Ferry D K, Akis R and Bird J P 2005 *J. Phys.: Condens. Matter* **17** S1017

[22] Deng Y X, Yan X H and Tang N S 2006 *Acta Phys. Sin.* **55** 2027 (in Chinese)

[23] Sun K W and Xiong S J 2006 *Chin. Phys.* **15** 0828

[24] M. van den Broek and Peeters F M 2001 *Physica* E **11** 345

[25] Waalkens H, Wiersig J and Dullin H R 1997 *Ann. Phys.* **260** 50

[26] Hou C F and Guo R H 2005 *Acta Phys. Sin.* **54** 1972 (in Chinese)

[27] Lundberg T 1994 *Comput. Mater. Sci.* **3** 78

[28] Kirczenow G 1988 *Phys. Rev.* B **39** 10452